Wavelet analysis on some surfaces of revolution via area preserving projection

Daniela Rosca*

September 30, 2010

Abstract

We give a simple method for constructing a projection from a surface of revolution $\mathcal{M}$ onto the plane perpendicular to the rotation axis, which preserves areas. Then we use this projection for constructing a multiresolution analysis and a continuous wavelet transform, starting from the existing planar constructions. Thus, the wavelets on $\mathcal{M}$ inherit all the properties of the corresponding planar wavelets.

Keywords: continuous wavelet transform (CWT), discrete wavelet transform (DWT), wavelet transform on manifolds, equal area projection.

1 Introduction

Real life signals often live on 2D curved manifolds, such as a sphere (geosciences), a paraboloid (optics), a two-sheeted hyperboloid (cosmology, optics) or a cone. In order to design approximation and analysis techniques on such surfaces, an efficient way is to exploit methods existent on domains of the plane $\mathbb{R}^2$. Such an approach requires an appropriate projection from the manifold onto $\mathbb{R}^2$. In a previous paper, we have explored this method systematically [3]. In particular, for the manifolds mentioned above, we have described the vertical and the stereographic projections. While these projections have nice properties, they suffer from one major drawback, namely, they do not preserve areas. As a consequence, lifting the DWT via the inverse projections results in severe distortions at large distances (e.g. close to the North Pole in the case of the sphere).

In Section 2 we present a simple method of constructing a projection which preserves the area. It applies to all 2D surfaces of revolution obtained by rotating a piecewise smooth plane curve around a line in its plane, such that one end point of the curve is the only point of intersection with the line and each plane perpendicular to the line intersects the curve at most once. In the sequel, we denote by $\mathcal{M}$ such a surface. For the construction of a multiresolution analysis of $L^2(\mathcal{M})$ and a CWT on $\mathcal{M}$ we also need to suppose that the curve that generates the surface has infinite length. Examples are the surfaces mentioned above. Applied to the sphere, our projection is in fact Lambert's azimuthal projection, which has a nice geometrical interpretation. However, the present method for constructing a CWT and DWT does not apply to the sphere. But a similar approach may be designed in the case when the generating curve has finite length (thus including the case of the sphere), based on a mapping from a square onto a disc, followed by a lifting to the sphere by inverse Lambert projection [10].

*Technical University of Cluj-Napoca, Department of mathematics, str. Memorandumului 38, RO-400114 Cluj-Napoca, Romania. Email: Daniela.Rosca@math.utcluj.ro

In this paper, we shall consider the case of a general surface of revolution, then particularize to the paraboloid, the upper sheet of the two-sheeted hyperboloid and the positive part of the cone, all axisymmetric. These three manifolds are the ones that are the most useful for applications. In optics, data on such manifolds are essential for the treatment of omnidirectional images via the catadioptric procedure, for instance in robotic vision. That last topic is particularly relevant for engineering purposes, because of the many applications in navigation, surveillance, visualization. In the catadioptric image processing, a sensor overlooks a mirror, whose shape may be spherical, hyperbolic or parabolic. However, instead of projecting the data from that mirror onto a plane, an interesting alternative consist in processing them directly on the mirror, and thus wavelets on such manifolds are needed [5]. Among the three shapes, the parabolic one is the most common (think of the headlights of a car).

Before proceeding, it is worth comparing our approach to the (scarce) existing literature. For the case of the hyperboloid $\mathcal{H}$, a CWT has been designed by Bogdanova *et al.* [4], using the group-theoretical approach translated from the corresponding (dual) case of the sphere and projection from $\mathcal{H}$ onto the tangent cone. In particular, the method starts from the $\mathrm{SO}_0(2,1)$ invariant metric on $\mathcal{M}$ and exploits the harmonic analysis on $\mathcal{M}$ provided by the Fourier-Helgason transform. However, the resulting CWT has not been discretized and no DWT is known. As for the paraboloid $\mathcal{P}$, there is no global isometry group, so that the group-theoretical method is not directly applicable. A tentative has been put forward by Honnouvo [7], but it is not really conclusive (and it is again limited to the continuous transform). Further comments on this approach may be found in [2].

In all these methods, the measure on $\mathcal{M}$ and the projection onto $\mathbb{R}^2$ are determined by geometry (group theory). However, the measure is not dilation invariant and the projection does not preserve areas, which forces one to introduce correction factors. In the method presented here, on the contrary, we start by calculating a projection $\mathcal{M} \to \mathbb{R}^2$ that does preserve area and is bijective. As a consequence, it induces a unitary map between $L^2(\mathcal{M})$ and $L^2(\mathbb{R}^2)$. Inverting the latter, we can then lift all operations from the plane to $\mathcal{M}$, in particular, producing unitary operators on $L^2(\mathcal{M})$ that implement translations, rotations and dilations in the plane. In this way, the representation of the similitude group of the plane, that underlines the 2D plane CWT, is lifted to $\mathcal{M}$ as well. Thus we have all the necessary ingredients for constructing a multiresolution analysis and a DWT on $\mathcal{M}$ (Section 3), that does not show distortions, because of the area preserving property. In the same way, we design a CWT on $\mathcal{M}$ (Section 4), with no need to use explicitly a given measure. In fact, all calculations are performed in the plane, not on $\mathcal{M}$, exploiting the unitarity of the map that links the corresponding L^2 spaces. This in a sense reverses the perspective and makes the method both simpler and more efficient.

2 Equal area projections from some surfaces of revolution onto OXY

In this section we present the construction of the projection preserving areas. Then we will give the expression of the projection and its inverse in the cases of the paraboloid, the upper sheet of two-sheeted hyperboloid and the positive part of the cone, since these cases are the most useful in practice.

2.1 Construction of the projection

Consider the surface of revolution

$$\mathcal{M}: \begin{cases} x = \rho\cos t, \\ y = \rho\sin t, \\ z = \varphi(\rho), \quad t \in [0, 2\pi), \ \rho \in I = [0, b) \text{ or } [0, \infty). \end{cases}$$

obtained by rotating the planar curve of equation $z = \varphi(x)$ around Oz. We suppose that $\varphi \geq 0$, φ is piecewise smooth and increasing on I.

Our goal is to construct a bijection p from $\mathcal{M}$ to a subset of the plane XOY which preserves the areas. More precisely, for every portion $\mathcal{S}$ of $\mathcal{M}$ we must have $\mathcal{A}(\mathcal{S}) = \mathcal{A}(\mathsf{p}(\mathcal{S}))$, where $\mathcal{A}(\mathcal{S})$ denotes the area of $\mathcal{S}$.

The intersection of $\mathcal{M}$ with the plane $z = z_0$, $z_0 \in \varphi(I), z_0 \neq 0$, will be a circle of radius $\rho_0 = \varphi^{-1}(z_0)$. In particular, if we consider the portion $\mathcal{M}_0$ situated under the plane $z = z_0$,

$$\mathcal{M}_0: \begin{cases} z = \varphi(\sqrt{x^2 + y^2}), \\ z \leq z_0, \end{cases}$$

then we must have $\mathcal{A}(\mathcal{M}_0) = \mathcal{A}(\mathsf{p}(\mathcal{M}_0))$. In fact, we calculate $\mathcal{A}(\mathcal{M}_0)$ and determine the radius R_0 of the circle with area equal to $\mathcal{A}(\mathcal{M}_0)$. Next, the projection $M' = \mathsf{p}(M)$ of a point $M(x, y, \varphi(\sqrt{x^2 + y^2})) \in \mathcal{M}$, $x, y \neq 0$, will be defined as follows (see Figure 1):

1. Consider $N(x, y, 0)$ the vertical projection of M;

2. Take M' on the half line ON, such that $OM' = R_0$.

In this way, the area of $\mathsf{p}(\mathcal{M}_0)$ will be πR_0^2, which is exactly $\mathcal{A}(\mathcal{M}_0)$.

So, let us calculate $\mathcal{A}(\mathcal{M}_0)$. We have

$$\mathcal{A}(\mathcal{M}_0) = \iint_{\mathcal{M}_0} dS = \int_0^{2\pi} dt \int_0^{\varphi^{-1}(z_0)} \sqrt{EG - F^2}\, d\rho,$$

with

$$\begin{aligned} E &= (x'_t)^2 + (y'_t)^2 + (z'_t)^2 = \rho^2, \\ F &= x'_t x'_\rho + y'_t y'_\rho + z'_t z'_\rho = 0, \\ G &= (x'_\rho)^2 + (y'_\rho)^2 + (z'_\rho)^2 = 1 + (\varphi'(\rho))^2. \end{aligned}$$

Next we have, with the notation $\rho_0 = \varphi^{-1}(z_0)$,

$$\mathcal{A}(\mathcal{M}_0) = \int_0^{2\pi} dt \int_0^{\rho_0} \rho\sqrt{1 + (\varphi'(\rho))^2}\, d\rho = \pi h(\rho_0),$$

where $h : I \to h(I) \subseteq [0, \infty)$ satisfies the equality

$$h'(\rho) = 2\rho\sqrt{1 + (\varphi'(\rho))^2}. \tag{1}$$

It is immediate that the function h is increasing and continuous, therefore bijective. The radius R_0 of the disc $\mathsf{p}(\mathcal{M}_0)$ is

$$R_0 = \sqrt{h(\rho_0)}.$$

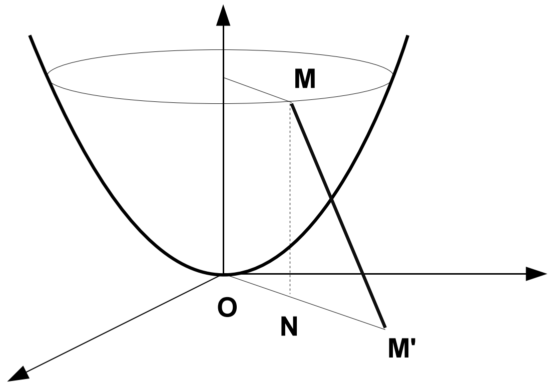

Figure 1: The projection M' of a point $M \in \mathcal{M}$.

If we denote by (X, Y) the coordinates of $M' \neq O$, then one can easily deduce that

$$X = R\cos t = \frac{x}{\rho}\sqrt{h(\rho)}, \quad (2)$$

$$Y = R\sin t = \frac{y}{\rho}\sqrt{h(\rho)} \cdot . \quad (3)$$

In the case when $\rho = 0$ we take $\mathsf{p}(0,0,f(0)) = (0,0)$.
In order to determine the inverse, we first observe that $X^2 + Y^2 = h(\rho)$, whence

$$\rho = h^{-1}(X^2 + Y^2).$$

Then, the inverse p^{-1} can be written as

$$x = \frac{X}{\sqrt{X^2+Y^2}}\, h^{-1}(X^2+Y^2), \quad (4)$$

$$y = \frac{Y}{\sqrt{X^2+Y^2}}\, h^{-1}(X^2+Y^2), \quad (5)$$

$$z = \varphi(h^{-1}(X^2+Y^2)). \quad (6)$$

Finally, we have to prove that our projection p preserves the areas. Indeed,

$$\begin{aligned} E &= (x'_X)^2 + (y'_X)^2 + (z'_X)^2 = Y^2 A^2(X,Y) + X^2 B(X,Y) \\ F &= x'_X x'_Y + y'_X y'_Y + z'_X z'_Y = XY(B(X,Y) - A^2(X,Y)) \\ G &= (x'_Y)^2 + (y'_Y)^2 + (z'_Y)^2 = X^2 A^2(X,Y) + Y^2 B(X,Y), \end{aligned}$$

with

$$\begin{aligned} A(X,Y) &= \frac{h^{-1}(X^2+Y^2)}{X^2+Y^2} = \frac{\rho}{h(\rho)}, \\ B(X,Y) &= \big(1 + (\varphi'(h^{-1}(X^2+Y^2)))^2\big)\big((h^{-1})'(X^2+Y^2)\big)^2 \\ &= \big(1+\varphi'(\rho)\big)\big((h^{-1})'(h(\rho))\big)^2 = \frac{1}{4\rho^2(1+(\varphi'(\rho))^2)}. \end{aligned}$$

The last equality was obtained from the relation

$$(h^{-1})'(h(\rho)) \cdot h'(\rho) = 1,$$

obtained from (1) and by differentiating the equality $h^{-1}(h(\rho)) = \rho$.

Then, a straightforward calculation gives that $EG - F^2 = 1$, so that indeed our projection p preserves the area. In the case when the curve defined by the function φ has infinite length, the area preserving property allows us to construct on $\mathcal{M}$ a uniform grid simply by lifting a uniform grid on the plane via p^{-1}. Thus we obtain the essential ingredient for defining a multiresolution analysis on $\mathcal{M}$, as will be done in Section 3.3.

2.2 Equal area projection from the paraboloid $a^2z = x^2 + y^2$ onto XOY

Consider the paraboloid $\mathcal{P} : z = (x^2 + y^2)/a^2$. We use the following parametrization of $\mathcal{P}_0$:

$$\mathcal{P}_0 : \begin{cases} x = a\rho\cos t \\ y = a\rho\sin t \\ z = \rho^2 \end{cases}, \quad t \in [0, 2\pi),\ \rho \in [0, \sqrt{z_0}\,].$$

We have

$$\begin{aligned} \mathcal{A}(\mathcal{P}_0) &= \int_0^{2\pi} dt \int_0^{\sqrt{z_0}} a\rho\sqrt{4\rho^2 + a^2}\, d\rho = 2\pi \cdot \frac{a}{12}(a^2 + 4\rho^2)^{3/2} \Big|_{\rho=0}^{\rho=\sqrt{z_0}} \\ &= \frac{a\pi}{6}\left((4z_0 + a^2)^{3/2} - a^2\right), \end{aligned}$$

and therefore the radius R_0 of the disc $\mathsf{p}(\mathcal{P}_0)$ is

$$R_0 = \sqrt{a \cdot \frac{(4z_0 + a^2)^{3/2} - a^2}{6}}.$$

For the projection p we deduce the formulas

$$X = R\cos t = \sqrt{\frac{(4z + a^2)^{3/2} - a^2}{6a}} \cdot \frac{x}{\sqrt{z}}, \tag{7}$$

$$Y = R\sin t = \sqrt{\frac{(4z + a^2)^{3/2} - a^2}{6a}} \cdot \frac{y}{\sqrt{z}}. \tag{8}$$

For the origin O we take $\mathsf{p}(O) = O$, that is $\mathsf{p}(0, 0, 0) = (0, 0)$.

The coordinates (x, y, z) of $M = \mathsf{p}^{-1}(\mathsf{M}')$, where $M' = M'(X, Y)$, are

$$x = \frac{a^{2/3}}{2} X \sqrt{\frac{(6X^2 + 6Y^2 + a^3)^{2/3} - a^{8/3}}{X^2 + Y^2}}, \tag{9}$$

$$y = \frac{a^{2/3}}{2} Y \sqrt{\frac{(6X^2 + 6Y^2 + a^3)^{2/3} - a^{8/3}}{X^2 + Y^2}}, \tag{10}$$

$$z = \frac{(6X^2 + 6Y^2 + a^3)^{2/3} - a^{8/3}}{4a^{2/3}}. \tag{11}$$

An example of uniform grid on $\mathcal{P}$ is given in Figure 2.

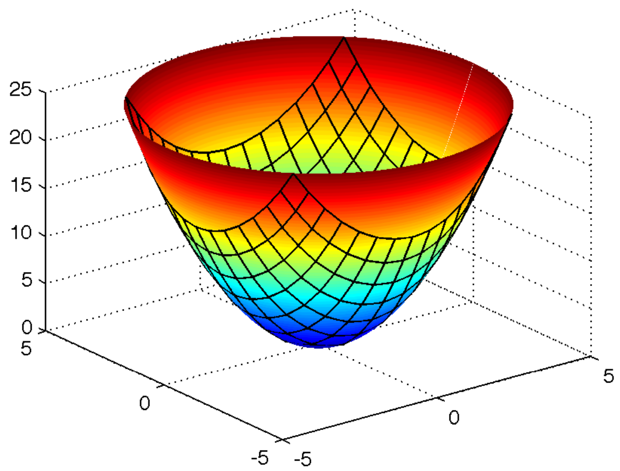

Figure 2: A uniform grid on the paraboloid $\mathcal{P} : z = x^2 + y^2$, formed by applying the projection p^{-1} given in (9)-(11) to the planar grid $G = \{x = -35 + 5i,\ i = 0, 1, \ldots, 14\} \cup \{y = -35 + 5j,\ j = 0, 1, \ldots, 14\}$.

2.3 Equal area projection from the hyperboloid $z = \sqrt{1 + (x^2 + y^2)/a^2}$ onto XOY

We consider the (upper sheet) of the hyperboloid, $\mathcal{H} : z = \sqrt{1 + (x^2 + y^2)/a^2}$, with $a > 0$, and we try to perform the same steps as before. The intersection of $\mathcal{H}$ with the plane $z = z_0, z_0 > 1$, is a circle of radius $r_0 = \sqrt{z_0^2 - 1}$. We calculate again the area of

$$\mathcal{H}_0 : \begin{cases} z = \sqrt{1 + \frac{x^2+y^2}{a^2}}, \\ z \leq z_0. \end{cases}$$

We use the parametric equations

$$\mathcal{H}_0 : \begin{cases} x = a\rho \cos t \\ y = a\rho \sin t \\ z = \sqrt{\rho^2 + 1} \end{cases}, \quad t \in [0, 2\pi),\ \ \rho \in [0, r_0].$$

We obtain, after simple calculations,

$$EG - F^2 = a^2 \rho^2 \frac{(a^2+1)\rho^2 + a^2}{\rho^2 + 1}$$

and further

$$\mathcal{A}(\mathcal{H}_0) = 2\pi \int_0^{r_0} a\rho \sqrt{\frac{(a^2+1)\rho^2 + a^2}{\rho^2 + 1}}\, d\rho = \frac{\pi}{2} f(r_0) = \frac{\pi}{2} g(z_0),$$

where $f : (0, \infty) \to \mathbb{R}$, $g : (1, \infty) \to \mathbb{R}$,

$$\begin{aligned} f(r) &= \frac{2}{\sqrt{a^2+1}} \log\left(\sqrt{(1+a^2)(1+r^2)} - \sqrt{a^2 + (1+a^2)r^2}\,\right) \\ &+ 2\sqrt{(1+r^2)(1+(1+a^2)r^2)} + \frac{2}{\sqrt{a^2+1}} \log(a + \sqrt{a^2+1}) - 2a, \end{aligned}$$

$$
\begin{aligned}
g(z) &= \frac{2}{\sqrt{1+a^2}} \log(z\sqrt{1+a^2} - \sqrt{(1+a^2)z^2-1}) \\
&+ 2z\sqrt{(1+a^2)z^2-1} + \frac{2}{\sqrt{a^2+1}} \log(a+\sqrt{1+a^2}) - 2a.
\end{aligned}
$$

In conclusion, the radius of the disc $\mathsf{p}(\mathcal{H}_0)$ is

$$
R_0 = \sqrt{\frac{g(z_0)}{2}}.
$$

Again, if we denote by (X, Y) the coordinates of $M' = \mathsf{p}(\mathsf{M})$, for $M(x, y, z) \in \mathcal{H}$, $M \neq (0, 0, 1)$, then one can easily deduce that

$$
X = R\cos t = \sqrt{\frac{g(z)}{2}} \cdot \frac{x}{a\sqrt{z^2-1}}, \tag{12}
$$

$$
Y = R\sin t = \sqrt{\frac{g(z)}{2}} \cdot \frac{y}{a\sqrt{z^2-1}}. \tag{13}
$$

The projection of $(0, 0, 1)$ is taken $(0, 0)$.

Unfortunately, in the case of the hyperboloid, an explicit expression for the inverse p^{-1} cannot be determined as for the paraboloid. Indeed, we have

$$
X^2 + Y^2 = \frac{g(z)}{2},
$$

and since we cannot have an explicit expression of g^{-1}, we cannot obtain z as an explicit function of $X^2 + Y^2$. However, we can solve numerically the nonlinear equation $g(z) = b$, for fixed $b > 0$, by applying the Newton-Raphson method or the secant method, since $g \in C^2[1, \infty)$ and both g' and g'' have constant sign.

The coordinates (x, y, z) of $M = \mathsf{p}^{-1}(\mathsf{M}')$, $M'(X, Y) \neq (0, 0)$, are

$$
x = aX\sqrt{\frac{\left(g^{-1}(2X^2+2Y^2)\right)^2 - 1}{X^2+Y^2}}, \tag{14}
$$

$$
y = aY\sqrt{\frac{\left(g^{-1}(2X^2+2Y^2)\right)^2 - 1}{X^2+Y^2}}, \tag{15}
$$

$$
z = g^{-1}(2X^2+2Y^2). \tag{16}
$$

An example of uniform grid on $\mathcal{H}$ is given in Figure 3.

2.4 Equal area projection from the conical surface $z = \sqrt{(x^2+y^2)/a^2}$ onto XOY

Consider the cone $\mathcal{C}$ of equation $z = \sqrt{(x^2+y^2)/a^2}$, with $a > 0$, and for the portion $\mathcal{C}_0$ with $z < z_0$ we use the parametric equations

$$
\mathcal{C}_0 : \begin{cases} x = a\rho\cos t \\ y = a\rho\sin t \\ z = \rho \end{cases}, \quad t \in [0, 2\pi),\ \rho \in [0, z_0].
$$

For the radius of the disc $\mathsf{p}(\mathcal{C}_0)$ we obtain

$$
R_0 = a^{1/2}(a^2+1)^{1/4} z_0,
$$

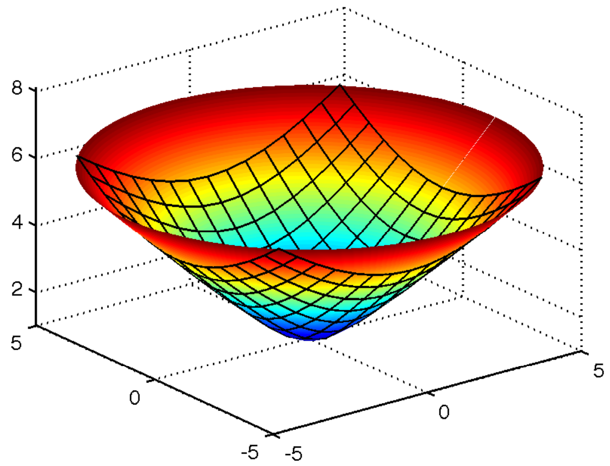

Figure 3: A uniform grid on the hyperboloid $\mathcal{H} : z = \sqrt{1+x^2+y^2}$, formed by applying the projection p^{-1} given in (14)-(16) to the planar grid $G = \{x = -5 + 5i/7,\ i = 0, 1, \ldots, 14\} \cup \{y = -35 + 5j/7,\ j = 0, 1, \ldots, 14\}$.

and for the projection p and its inverse we obtain, respectively

$$\begin{aligned} X &= R\cos t = a^{1/2}(a^2+1)^{1/4} z \cdot \frac{x}{az} = x\, a^{-1/2}(a^2+1)^{1/4}, \\ Y &= R\sin t = a^{1/2}(a^2+1)^{1/4} z \cdot \frac{y}{az} = y\, a^{-1/2}(a^2+1)^{1/4} \end{aligned}$$

and

$$x = a^{1/2}(a^2+1)^{-1/4} X \tag{17}$$
$$y = a^{1/2}(a^2+1)^{-1/4} Y \tag{18}$$
$$z = a^{-1/2}(a^2+1)^{-1/4}\sqrt{X^2+Y^2}. \tag{19}$$

An example of uniform grid on $\mathcal{C}$ is given in Figure 4.

3 Multiresolution analysis of $L^2(\mathcal{M})$

3.1 Functions in $L^2(\mathcal{M})$

We will restrict ourselves to the case when the generating curve φ has infinite length. Let $\mathcal{M}$ be the surface of revolution considered before, given by the parametric equations

$$\xi = \xi(X, Y) = (x(X, Y), y(X, Y), z(X, Y)), \quad (X, Y) \in \mathbb{R}^2,$$

where the expressions of x, y, z are given in (9)-(11) for the paraboloid, (14)-(16) for the hyperboloid and (17)-(19) for the cone. We also consider the projection $\mathsf{p} : \mathcal{M} \to \mathbb{R}^2$ described in Section 2. This projection is obviously bijective and its inverse is $\mathsf{p}^{-1} : \mathbb{R}^2 \to \mathcal{M}$,

$$\mathsf{p}^{-1}(X, Y) = \xi(X, Y) = (x(X, Y), y(X, Y), z(X, Y)).$$

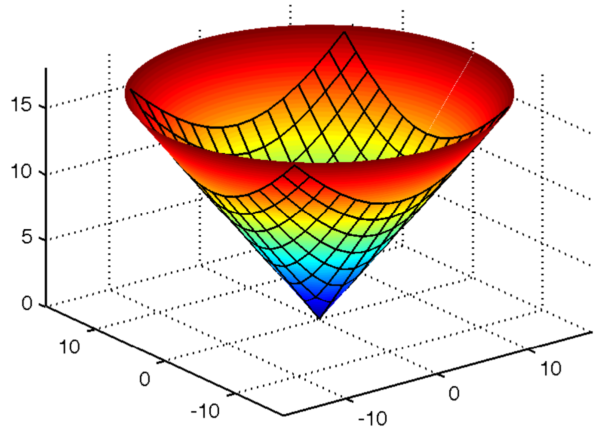

Figure 4: A uniform grid on the cone $\mathcal{C} : z = \sqrt{x^2 + y^2}$, formed by applying the projection p^{-1} given in (17)-(19) to the planar grid $G = \{x = -5 + 5i/7,\ i = 0, 1, \ldots, 14\} \cup \{y = -35 + 5j/7,\ j = 0, 1, \ldots, 14\}$.

We have seen in Section 2 that p preserves the area, so that the area element $d\omega(\xi)$ of $\mathcal{M}$ equals the element area $dXdY = d\mathbf{x}$ of $\mathbb{R}^2$. Therefore, for all $\widetilde{f}, \widetilde{g} \in L^2(\mathcal{M})$ we have

$$\begin{aligned} \langle \widetilde{f}, \widetilde{g} \rangle_{L^2(\mathcal{M})} &= \int_{\mathcal{M}} \overline{\widetilde{f}(\xi)} \widetilde{g}(\xi) d\omega(\xi) \\ &= \int_{\mathsf{p}(\mathcal{M})} \overline{\widetilde{f}(\mathsf{p}^{-1}(X,Y))} \widetilde{g}(\mathsf{p}^{-1}(X,Y))\, dX dY \\ &= \langle \widetilde{f} \circ \mathsf{p}^{-1}, \widetilde{g} \circ \mathsf{p}^{-1} \rangle_{L^2(\mathbb{R}^2)} \end{aligned} \tag{20}$$

and similarly, for all $f, g \in L^2(\mathbb{R}^2)$ we have

$$\langle f, g \rangle_{L^2(\mathbb{R}^2)} = \langle f \circ \mathsf{p}, g \circ \mathsf{p} \rangle_{L^2(\mathcal{M})}. \tag{21}$$

Consider now the map $\Pi : L^2(\mathcal{M}) \to L^2(\mathbb{R}^2)$, induced by the projection p, defined by

$$(\Pi \widetilde{f})(X, Y) = \widetilde{f}(\mathsf{p}^{-1}(X, Y)), \text{ for all } \widetilde{f} \in L^2(\mathcal{M}).$$

Its inverse $\Pi^{-1} : L^2(\mathbb{R}^2) \to L^2(\mathcal{M})$ is

$$(\Pi^{-1} f)(\xi) = f(\mathsf{p}(\xi)), \quad \text{for all } f \in L^2(\mathbb{R}^2).$$

From equalities (20) and (21) it follows that Π is a unitary map, that is,

$$\begin{aligned} \langle \Pi \widetilde{f}, \Pi \widetilde{g} \rangle_{L^2(\mathbb{R}^2)} &= \langle \widetilde{f}, \widetilde{g} \rangle_{L^2(\mathcal{M})}, \\ \langle \Pi^{-1} f, \Pi^{-1} g \rangle_{L^2(\mathcal{M})} &= \langle f, g \rangle_{L^2(\mathbb{R}^2)}. \end{aligned}$$

Equality (21) is the key equality of this paper. It allows us to establish the following results, whose proof is immediate:

Proposition 1 *Let J be a countable set and let $\{f_k\}_{k\in J} \subseteq L^2(\mathbb{R}^2)$. For each $k \in J$ we define $\widetilde{f_k} \in L^2(\mathcal{M})$ as $\widetilde{f_k} = f_k \circ \mathsf{p}$. Then we have:*

1. *If $\{f_k\}_{k\in J}$ is an orthonormal basis of $L^2(\mathbb{R}^2)$, then $\{\widetilde{f_k}\}_{k\in J}$ is an orthonormal basis of $L^2(\mathcal{M})$;*

2. *If $\{f_k\}_{k\in J}$ is a Riesz basis of $L^2(\mathbb{R}^2)$ with Riesz constants A, B, then $\{\widetilde{f_k}\}_{k\in J}$ is a Riesz basis of $L^2(\mathcal{M})$ with the same Riesz constants;*

3. *If $\{f_k\}_{k\in J}$ is a frame of $L^2(\mathbb{R}^2)$ with frame bounds A, B, then $\{\widetilde{f_k}\}_{k\in J}$ is a frame of $L^2(\mathcal{M})$ with the same frame bounds.*

3.2 Multiresolution analysis (MRA) and wavelet bases of $L^2(\mathbb{R}^2)$

In order to fix our notations, we will briefly review in this section the standard construction of 2-D orthonormal wavelet bases in the flat case, starting from a multiresolution analysis (MRA) [8].

Let D be a 2×2 regular matrix with the properties

(a) $D\mathbb{Z}^2 \subset \mathbb{Z}^2$, which is equivalent to the fact that D has integer entries,

(b) $\lambda \in \sigma(D) \Longrightarrow |\lambda| > 1$, that is, all eigenvalues of D have modulus greater than 1.

A multiresolution analysis of $L^2(\mathbb{R}^2)$ associated to D is an increasing sequence of closed subspaces $\mathbf{V}_j \subset L^2(\mathbb{R}^2)$ with $\bigcap_{j\in\mathbb{Z}} \mathbf{V}_j = \{0\}$ and $\overline{\bigcup_{j\in\mathbb{Z}} \mathbf{V}_j} = L^2(\mathbb{R}^2)$, and satisfying the following conditions:

(1) $f \in \mathbf{V}_j \iff f(D\,\cdot) \in \mathbf{V}_{j+1}$,

(2) There exists a function $\Phi \in L^2(\mathbb{R}^2)$ such that the set $\{\Phi(\cdot - \mathbf{k}),\ \mathbf{k} \in \mathbb{Z}^2\}$ is an orthonormal basis of $\mathbf{V}_0$.

As a consequence, $\{\Phi_{j,\mathbf{k}} := |\det D|^{j/2}\Phi(D^j \cdot -\mathbf{k}),\ \mathbf{k} \in \mathbb{Z}^2\}$ is an orthonormal basis for $\mathbf{V}_j$.

For each $j \in \mathbb{Z}$, let us define the space $\mathbf{W}_j$ as the orthogonal complement of $\mathbf{V}_j$ into $\mathbf{V}_{j+1}$, i.e., $\mathbf{V}_{j+1} = \mathbf{V}_j \oplus \mathbf{W}_j$. The two-dimensional wavelets are those functions which span $\mathbf{W}_0$. One can prove (see [9]) that there exist $q = |\det D| - 1$ wavelets ${}^1\Psi, {}^2\Psi, \ldots, {}^q\Psi \in \mathbf{V}_1$ that generate an orthonormal basis of $\mathbf{W}_0$. Therefore, $\{{}^\lambda\Psi_{j,\mathbf{k}} := |\det D|^{j/2} \cdot {}^\lambda\Psi(D^j \cdot -\mathbf{k}),\ \lambda = 1, \ldots, q,\ \mathbf{k} \in \mathbb{Z}^2\}$ is an orthonormal basis of $\mathbf{W}_j$ for each j, and $\{{}^\lambda\Psi_{j,\mathbf{k}},\ \lambda = 1, \ldots, q,\ \mathbf{k} \in \mathbb{Z}^2,\ j \in \mathbb{Z}\}$ is an orthonormal basis of $L^2(\mathbb{R}^2)$.

A particular case is that of tensor product wavelets, corresponding to the dilation matrix $D = \mathrm{diag}\,[2, 2]$ and a 1-D MRA with scaling function and mother wavelet ϕ, ψ. In this case, $q = 3$ and one gets the 2-D scaling function $\Phi(x, y) = \phi(x)\phi(y)$ and the three wavelets

$$ {}^h\Psi(x, y) = \phi(x)\psi(y), \quad {}^v\Psi(x, y) = \psi(x)\phi(y), \quad {}^d\Psi(x, y) = \psi(x)\psi(y). $$

If the one-dimensional functions ϕ and ψ have compact support, then obviously so have Φ and ${}^\lambda\Psi$. This is the case of the well-known Daubechies wavelets.

3.3 Multiresolution analysis and orthonormal wavelet bases of $L^2(\mathcal{M})$

The construction of multiresolution analysis and wavelet bases in $L^2(\mathcal{M})$ is based on the equality (21). To every function $f \in L^2(\mathbb{R}^2)$, one can associate the function $f^{\mathcal{M}} \in L^2(\mathcal{M})$ as

$$ f^{\mathcal{M}} = f \circ \mathsf{p}. \tag{22} $$

In particular, if the functions $\{f_{j,\mathbf{k}}\}_{j,\mathbf{k}}$ are orthogonal, so are

$$f^{\mathcal{M}}_{j,\mathbf{k}} = f_{j,\mathbf{k}} \circ \mathsf{p}, \ \text{for } j \in \mathbb{Z},\ \mathbf{k} \in \mathbb{Z}^2. \tag{23}$$

Then, taking $f = \Phi$ and $f = \Psi$, we obtain the functions on $\mathcal{M}$

$$\Phi^{\mathcal{M}}_{j,\mathbf{k}} = \Phi_{j,\mathbf{k}} \circ \mathsf{p}, \quad {}^{\lambda}\Psi^{\mathcal{M}}_{j,\mathbf{k}} = {}^{\lambda}\ \Psi_{j,\mathbf{k}} \circ \mathsf{p}. \tag{24}$$

For $j \in \mathbb{Z}$, we define the spaces $\mathcal{V}_j$ as

$$\mathcal{V}_j = \{f \circ \mathsf{p},\ f \in \mathbf{V}_j\}. \tag{25}$$

Using (21) and the unitarity of the map Π, it is immediate that $\mathcal{V}_j$ is a closed subspace of $L^2(\mathcal{M})$, thus a Hilbert space. Moreover, these spaces have the following properties:

(1) $\mathcal{V}_j \subset \mathcal{V}_{j+1}$ for $j \in \mathbb{Z}$,

(2) $\bigcap_{j\in\mathbb{Z}} \mathcal{V}_j = \{0\}$ and $\overline{\bigcup_{j\in\mathbb{Z}} \mathcal{V}_j} = L^2(\mathcal{M})$,

(3) The set $\{\Phi^{\mathcal{M}}_{0,\mathbf{k}},\ \mathbf{k} \in \mathbb{Z}^2\}$ is an orthonormal basis for $\mathcal{V}_0$.

We will say that a sequence of subspaces of $L^2(\mathcal{M})$ with the properties above constitutes a *multiresolution analysis* of $L^2(\mathcal{M})$.

Once the multiresolution analysis is determined, we construct the wavelet spaces $\mathcal{W}_j$ in the usual manner. Let $\mathcal{W}_j$ denote the orthogonal complement of the coarse space $\mathcal{V}_j$ in the fine space $\mathcal{V}_{j+1}$, so that

$$\mathcal{V}_{j+1} = \mathcal{V}_j \oplus \mathcal{W}_j.$$

One can easily prove that, for each $j \in \mathbb{Z}$, $\{{}^{\lambda}\Psi^{\mathcal{M}}_{j,\mathbf{k}},\ \mathbf{k} \in \mathbb{Z}^2, \lambda = 1,\ldots,q\}$ is an orthogonal basis for $\mathcal{W}_j$ and therefore $\{{}^{\lambda}\Psi^{\mathcal{M}}_{j,\mathbf{k}},\ j \in \mathbb{Z},\ \mathbf{k} \in \mathbb{Z}^2,\ \lambda = 1,\ldots,q\}$ is an orthonormal basis for $\overline{\bigoplus_{j\in\mathbb{Z}} \mathcal{W}_j} = L^2(\mathcal{M})$.

The conclusion of the analysis may be summarized as follows:

· If Φ has compact support in $\mathbb{R}^2$, then $\Phi^{\mathcal{M}}_{j,\mathbf{k}}$ has *compact support* on $\mathcal{M}$ (indeed diam supp $\Phi^{\mathcal{M}}_{j,\mathbf{k}} \to 0$ as $j \to \infty$).

· An *orthonormal/Riesz* 2-D wavelet basis leads to an *orthonormal/Riesz* basis of wavelets on $\mathcal{M}$.

· *Smooth* 2-D wavelets lead to *smooth* wavelets on $\mathcal{M}$, if the curve that generates the surface is smooth.

· In particular, plane tensor product Daubechies wavelets lead to locally supported and orthonormal wavelets on $\mathcal{M}$, and so do plane tensor product Haar wavelets.

· The decomposition and reconstruction matrices needed in the case of $\mathcal{M}$ are the same as in the plane 2-D case, so that the latter can be used (with existing toolboxes).

4 Continuous wavelet transform on $\mathcal{M}$

The construction of the CWT on $\mathcal{M}$ follows naturally from the CWT in the 2D case. So let us remind the 2D CWT [1].

In order to describe the motions in $\mathbb{R}^2$, one uses the following unitary operators in the space $L^2(\mathbb{R}^2)$:

(a) translation: $(T_{\mathbf{b}}s)(\mathbf{x}) = s(\mathbf{x}-\mathbf{b}),\ \mathbf{b}\in\mathbb{R}^2$;

(b) dilation: $(D_a s)(\mathbf{x}) = a^{-1}s(a^{-1}\mathbf{x}),\ a>0$;

(c) rotation: $(R_\theta s)(\mathbf{x}) = s(r_{-\theta}(\mathbf{x})),\ \theta\in[0,2\pi)$,

where $s\in L^2(\mathbb{R}^2)$ and r_θ is the rotation matrix

$$r_\theta = \begin{pmatrix} \cos\theta & -\sin\theta \\ \sin\theta & \cos\theta \end{pmatrix}.$$

Combining the three operators, we define the unitary operator

$$U(\mathbf{b},a,\theta) = T_{\mathbf{b}}D_aR_\theta,$$

which acts on a given function s as

$$[U(\mathbf{b},a,\theta)s](\mathbf{x}) = s_{\mathbf{b},a,\theta}(\mathbf{x}) = a^{-1}s(a^{-1}r_{-\theta}(\mathbf{x}-\mathbf{b})).$$

Their analogues on $\mathcal{M}$ will be defined as follows: We define the following unitary operators in the space $L^2(\mathcal{M})$:

(a) translation: $(\mathcal{T}_{\mathbf{b}}\widetilde{s})(\eta) := T_{\mathbf{b}}(\widetilde{s}\circ\mathsf{p}^{-1})(\mathsf{p}(\eta)) = (\widetilde{s}\circ\mathsf{p}^{-1})(\mathsf{p}(\eta)-\mathbf{b}),\ \mathbf{b}\in\mathbb{R}^2$;

(b) dilation: $(\mathcal{D}_a\widetilde{s})(\eta) := D_a(\widetilde{s}\circ\mathsf{p}^{-1})(\mathsf{p}(\eta)) = a^{-1}(\widetilde{s}\circ\mathsf{p}^{-1})(a^{-1}\mathsf{p}(\eta)),\ a>0$;

(c) rotation: $(\mathcal{R}_\theta\widetilde{s})(\eta) := R_\theta(\widetilde{s}\circ\mathsf{p}^{-1})(\mathsf{p}(\eta)) = (\widetilde{s}\circ\mathsf{p}^{-1})(\widetilde{r}_{-\theta}(\mathsf{p}(\eta))) = \widetilde{s}(\widetilde{r}_{-\theta}(\eta)),\ \theta\in[0,2\pi)$,

where $\widetilde{s}\in L^2(\mathcal{M})$, $\eta\in\mathcal{M}$ and $\widetilde{r}_\theta$ is the rotation matrix around Oz

$$\widetilde{r}_\theta = \begin{pmatrix} \cos\theta & -\sin\theta & 0 \\ \sin\theta & \cos\theta & 0 \\ 0 & 0 & 1 \end{pmatrix}.$$

Their combination gives rise to the operator $\mathcal{U}(\mathbf{b},a,\theta) = \mathcal{T}_{\mathbf{b}}\mathcal{D}_a\mathcal{R}_\theta$, which can be written as

$$[\mathcal{U}(\mathbf{b},a,\theta)\widetilde{s}](\eta) = a^{-1}(\widetilde{s}\circ\mathsf{p}^{-1})(a^{-1}r_\theta(p(\eta)-\mathbf{b})).$$

These operators on $L^2(\mathcal{M})$ are also unitary, as follows from the unitarity of the map Π.

A wavelet Ψ on $\mathbb{R}^2$ is defined as a function in $L^2(\mathbb{R}^2)$ satisfying the admissibility condition

$$C_\Psi := (2\pi)^2\int_{\mathbb{R}^2}\frac{|\widehat{\Psi}(\mathbf{y})|^2}{|\mathbf{y}|^2}d\mathbf{y} < \infty,$$

where the Fourier transform $\widehat{\Psi}$ of Ψ is defined as

$$\widehat{\Psi}(\mathbf{y}) = \frac{1}{2\pi}\int_{\mathbb{R}^2} e^{i\mathbf{x}\cdot\mathbf{y}}\Psi(\mathbf{x})d\mathbf{x}.$$

The question now is how to define a Fourier transform on $L^2(\mathcal{M})$ and an admissible wavelet in $L^2(\mathcal{M})$. The natural way to define the Fourier transform of a signal $\widetilde{s} \in L^2(\mathcal{M})$ is the following:

$$\begin{aligned}
\widehat{\widetilde{s}}(\eta) &:= \widehat{\widetilde{s} \circ \mathsf{p}^{-1}}(\mathsf{p}(\eta)) \\
&= \frac{1}{2\pi} \int_{\mathbb{R}^2} e^{-i\mathsf{p}(\eta)\cdot \mathbf{x}} (\widetilde{s} \circ \mathsf{p}^{-1})(\mathbf{x}) d\mathbf{x} \\
&= \frac{1}{2\pi} \int_{\mathcal{M}} e^{-i\mathsf{p}(\eta)\cdot \mathsf{p}(\xi)} \widetilde{s}(\xi) d\omega(\xi).
\end{aligned} \tag{26}$$

The last equality was obtained by writing $\mathbf{x} = \mathsf{p}(\xi)$, with $\xi \in \mathcal{M}$, and by taking into account the equality $d\mathbf{x} = d\omega(\xi)$, proved in Section 2.

Further, for the constant C_Ψ we obtain

$$\begin{aligned}
C_\Psi &= (2\pi)^2 \int_{\mathbb{R}^2} \frac{|\widehat{\Psi}(\mathbf{y})|^2}{|\mathbf{y}|^2} d\mathbf{y} = \int_{\mathcal{M}} \frac{|(\widehat{\Psi} \circ \mathsf{p})(\xi)|^2}{|\mathsf{p}(\xi)|^2} d\omega(\xi) \\
&= \int_{\mathcal{M}} \frac{|\widehat{(\Psi \circ \mathsf{p})}(\xi)|^2}{l^2(\xi)} d\omega(\xi).
\end{aligned}$$

In the first equality we put $\mathbf{y} = \mathsf{p}(\xi)$ and in the second we used the definition (26) for $\widetilde{s} \circ \mathsf{p}^{-1} = \Psi$. By $l(\xi)$ we have denoted the length of the curve $\widetilde{O\xi} = \mathsf{p}^{-1}(\overline{OM'}) \subset \mathcal{M}$, $\overline{OM'}$ being the segment with endpoints O and $M' = \mathsf{p}(\xi)$.

Thus, we can define a *wavelet* $\Psi^{\mathcal{M}}$ in $L^2(\mathcal{M})$ either by $\Psi^{\mathcal{M}} = \Psi \circ \mathsf{p}$, with Ψ a wavelet in $L^2(\mathbb{R}^2)$, or, equivalently, if it satisfies the admissibility condition

$$C_{\Psi^{\mathcal{M}}} = C_\Psi = \int_{\mathcal{M}} \frac{|\widehat{(\Psi \circ \mathsf{p})}(\xi)|^2}{l^2(\xi)} d\omega(\xi) < \infty.$$

We can now proceed to the definition of CWT for functions in $L^2(\mathcal{M})$. In the 2D case, one defines

$$\begin{aligned}
\Psi_{\mathbf{b},a,\theta} &= U(\mathbf{b}, a, \theta)\Psi, \text{ with } (\mathbf{b}, a, \theta) \in \mathcal{G}, \\
\mathcal{G} &= \{(\mathbf{b}, a, \theta), \quad \mathbf{b} \in \mathbb{R}^2,\, a > 0,\, \theta \in [0, 2\pi)\},
\end{aligned}$$

and one can prove (see [1], p. 35) that the set

$$\text{span}\{\Psi_{\mathbf{b},a,\theta},\ (\mathbf{b}, a, \theta) \in \mathcal{G}\}$$

is dense in $L^2(\mathbb{R}^2)$. Then, the CWT of a signal $s \in L^2(\mathbb{R}^2)$ with respect to the wavelet Ψ is defined as

$$(W_\Psi s)(\mathbf{b}, a, \theta) := \langle \Psi_{\mathbf{b},a,\theta}, s \rangle_{L^2(\mathbb{R}^2)}.$$

For a wavelet $\Psi^{\mathcal{M}}$, we will define, for $(\mathbf{b}, a, \theta) \in \mathcal{G}$, the functions

$$\Psi^{\mathcal{M}}_{\mathbf{b},a,\theta} := \mathcal{U}(\mathbf{b}, a, \theta)\Psi^{\mathcal{M}}.$$

These functions will also satisfy the admissibility condition, so that they are also wavelets. Moreover, simple calculations show that the set

$$\text{span}\{\Psi^{\mathcal{M}}_{\mathbf{b},a,\theta},\ (\mathbf{b}, a, \theta) \in \mathcal{G}\}$$

is dense in $L^2(\mathcal{M})$.

Finally, we can give the definition of CWT on $\mathcal{M}$.

Definition 2 *Given a wavelet $\Psi^{\mathcal{M}}$ and a signal $\widetilde{s} \in L^2(\mathcal{M})$, the continuous wavelet transform of $\widetilde{s}$ with respect to the wavelet $\Psi^{\mathcal{M}}$ is defined as*

$$(\mathcal{W}_{\Psi^{\mathcal{M}}}\, \widetilde{s})(\mathbf{b}, a, \theta) := \langle \Psi^{\mathcal{M}}_{\mathbf{b},a,\theta}, \widetilde{s}\,\rangle_{L^2(\mathcal{M})}.$$

This CWT can also be written as

$$\begin{aligned}(\mathcal{W}_{\Psi^{\mathcal{M}}}\, \widetilde{s})(\mathbf{b}, a, \theta) &= \langle \Psi^{\mathcal{M}}_{\mathbf{b},a,\theta}, \widetilde{s}\,\rangle_{L^2(\mathcal{M})} \\ &= \langle \mathcal{U}(\mathbf{b}, a, \theta)\Psi^{\mathcal{M}}, \widetilde{s}\,\rangle_{L^2(\mathcal{M})} \\ &= \langle U(\mathbf{b}, a, \theta)(\Psi^{\mathcal{M}} \circ \mathsf{p}^{-1}, \widetilde{s} \circ \mathsf{p}^{-1}\,\rangle_{L^2(\mathbb{R}^2)} \\ &= \langle \Psi_{\mathbf{b},a,\theta}, s\,\rangle_{L^2(\mathbb{R}^2)} \\ &= (W_\Psi s)(\mathbf{b}, a, \theta).\end{aligned}$$

By performing a composition with p on the right in the reconstruction formula for the 2D case, the following reconstruction formula holds in $L^2(\mathcal{M})$:

$$\widetilde{s}(\eta) = C^{-1}_{\Psi^{\mathcal{M}}} \iiint_J \Psi^{\mathcal{M}}_{\mathbf{b},a,\theta}(\eta)(\mathcal{W}_{\Psi^{\mathcal{M}}}\, \widetilde{s}\,)(\mathbf{b}, a, \theta)\, d\mathbf{b}\, \frac{da}{a^3} d\theta.$$

Finally, let us mention that any discretization of the 2D CWT can be moved onto $\mathcal{M}$, preserving the stability properties.

Conclusion

The approach presented in this paper allows us to move *any* construction of wavelets defined on $\mathbb{R}^2$ to a surface of revolution $\mathcal{M}$, which is piecewise smooth and has infinite area. Although the equal area projection p that we have described in Section 2 has no nice geometrical interpretation as the Lambert azimuthal projection, this is not important for implementations, as long as we have explicit formulas for p. Moreover, through this approach, the numerical behavior of planar 2D wavelets is inherited by the wavelets on $\mathcal{M}$. This implies, in particular, that both CWT and DWT on $\mathcal{M}$ have the same properties as the usual, planar ones. For this reason, we consider that there is no need to present particular examples. Finally we note that the definition of the continuous Fourier transform on $\mathcal{M}$ given in formula (26) can be used for defining a much simpler discrete Fourier transform than the one in [6].

Acknowledgement

The work has been co-funded by the Sectoral Operational Programme Human Resources Development 2007-2013 of the Romanian Ministry of Labor, Family and Social Protection through the Financial Agreement POSDRU/89/1.5/S/62557 and by the grant 436 RUM 113/31/0-1 of the German Research Foundation (DFG). Both are gratefully acknowledged.

References

[1] J.P. Antoine, R. Murenzi, P. Vandergheynst, S.T. Ali, *Two-Dimensional Wavelets and their Relatives*, Cambridge University Press, Cambridge, UK, 2004.

[2] J-P. Antoine, I. Bogdanova, and P. Vandergheynst, *The continuous wavelet transform on conic sections,* Int. J. Wavelets, Multires. and Inform. Proc. **6** (2007) 137–156.

[3] J.P. Antoine, D. Roşca, P. Vandergheynst, *Wavelet transform on manifolds: old and new approaches,* Appl. Comput. Harmon. Anal. 28 (2010), 189–202.

[4] I. Bogdanova, P. Vandergheynst, J.P. Gazeau, *Continuous wavelet transform on the hyperboloid,* Appl. Comput. Harmon. Anal. 23 (2007), 285–306.

[5] I. Bogdanova, X. Bresson, J.-Ph. Thiran, P. Vandergheynst, *Scale space analysis and active contours for omnidirectional images*, IEEE Trans. Image Process. **16** (7) (2007), 1888-1901.

[6] M. Calixto, J. Guerrero, J.C. Sánchez-Monreal, *Sampling theorem and discrete Fourier transform on the hyperboloid,* preprint arXiv: 0904.4716v1, 2009.

[7] G. Honnouvo, *Gabor Analysis and Wavelet Transforms on some Non-Euclidean 2-Dimensional Manifolds*, PhD Thesis, Concordia Univ., Montreal, PQ, Canada, 2007.

[8] A. Louis, P. Maass, and A. Rieder, *Wavelets, Theory and Applications*, Wiley, Chichester, 1997.

[9] Y. Meyer, *Wavelets and Operators*, Cambridge Studies in Advanced Mathematics, vol. 37, Cambridge University Press, Cambridge, UK, 1992.

[10] D. Roşca, *New uniform grids on the sphere*, Astronomy & Astrophysics, 2010, to appear.